1996 IEEE INTERNATIONAL FREQUENCY CONTROL SYMPOSIUM

THE FUNDAMENTAL NATURE OF ACCELERATION SENSITIVITY

John A. Kosinski*
U.S. Army Communications-Electronics Command
ATTN: AMSEL-RD-IEW-TAE-M
Fort Monmouth, NJ 07703

Abstract

In this paper, the fundamental nature of acceleration sensitivity is reviewed and clarified. The driving factor behind the acceleration-induced frequency shift is shown to be the deformation of the resonator. The deformation drives two effects: an essentially linear change in the frequency determining dimensions of the resonator, and an essentially nonlinear effect of changing the velocity of the propagating wave. The basic properties of acceleration sensitivity are illustrated through the simple examples of "BAW in a box" and "STW in a box". These examples serve to clarify a number of concepts, including the role of mode shape and the basic difference between the bulk acoustic wave and acoustic surface wave cases. Finally, these basic understandings are extended to other cases such as BAW microresonators.

* Currently on detail assignment to: U.S. Army Research Laboratory, AMSRL-PS-ED, Fort Monmouth, NJ 07703

Introduction

With the advent of modern personal satellite communications systems, acceleration sensitivity has transitioned from being a military-specific technology barrier to an important specification of commercial hardware. In this paper, the fundamental nature of acceleration sensitivity is reviewed and clarified.

The vast majority of communications systems maintain phase coherence through the use of low-noise crystal oscillators. Commercial off-the-shelf crystal oscillators are capable of meeting nearly all systems requirements, provided that the systems are at rest.

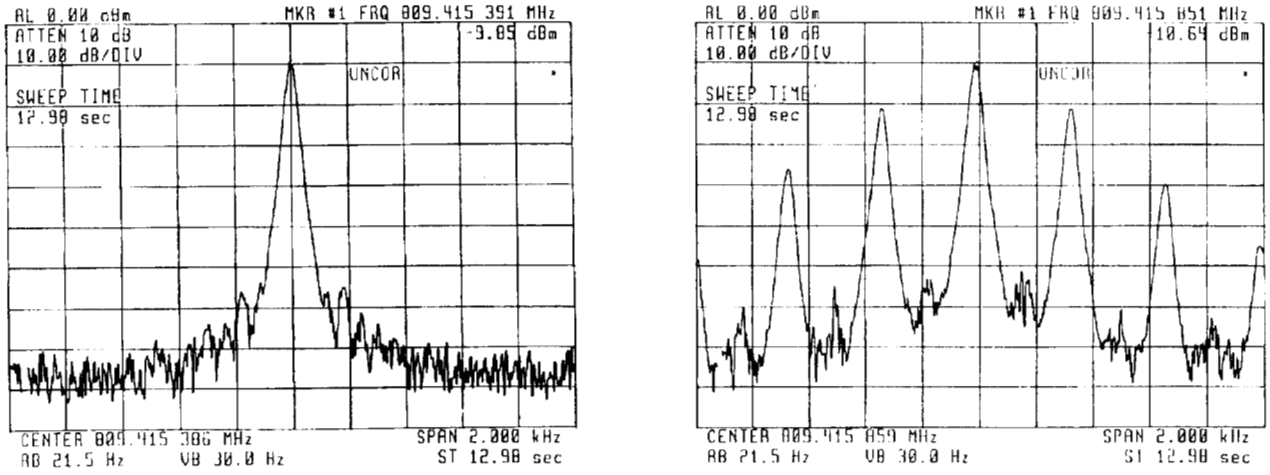

a) b)

Fig. 1. Output spectrum of a commercially available 809 MHz oscillator a) at rest and b) when subjected to a 1g sinusoidal vibration at 330 Hz.

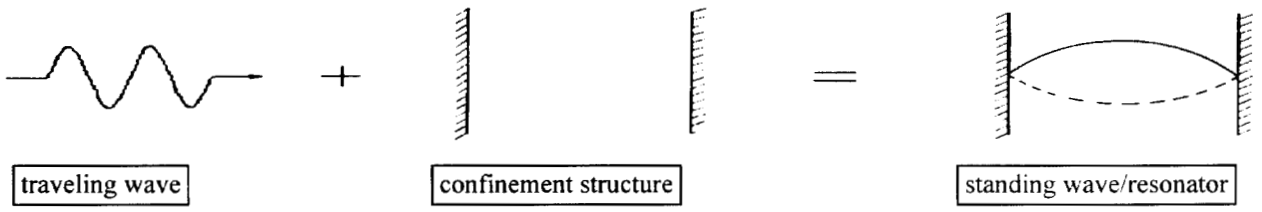

Fig. 2. Basic principle of operation of a generic resonator.

However, the noise output of the crystal oscillator is increased and the capabilities of the corresponding electronic systems are decreased by environmental vibrations encountered when, for example, the system is in motion. The magnitude of this problem is illustrated in Figure 1 wherein the output of a commercially available 809 MHz crystal oscillator is shown a) at rest and b) when the oscillator is subjected to a 1g sinusoidal vibration at 330 Hz. This phenomenon, known as "acceleration sensitivity", translates directly into increased bit error rates for mobile communications systems.

The problem of acceleration sensitivity in low-noise crystal oscillators was first seriously examined during the 1960's. Since then, the problem has been extensively studied by a wide variety of researchers in the military, industrial, and academic communities. However, it is only within the past several years that a clear understanding of the phenomenon has emerged.

Fundamental Nature

A typical low-noise oscillator uses a crystal resonator as the frequency determining element. An understanding of the fundamental nature of acceleration sensitivity in crystal oscillators resides primarily in understanding the acceleration sensitivity of the crystal resonator.

Components of the Acceleration-Induced Frequency Shift

The basic principle of operation of a generic resonator is shown in Figure 2. A traveling wave is combined with a confinement structure to produce a standing wave whose frequency is determined jointly by the velocity of the traveling wave and the dimensions of the confinement structure. In the case of crystal resonators, the traveling wave is either a bulk acoustic wave propagating through the interior of a piezoelectric crystal substrate or an acoustic surface wave propagating on the surface of a piezoelectric crystal substrate. In the case of bulk acoustic wave (BAW) resonators, the wave is confined by the substrate surfaces, while in the case of acoustic surface wave resonators, the wave is confined by metal-strip Fabry-Perot reflectors deposited on the propagation surface.

Given that the frequency of the crystal resonator is determined jointly by the velocity of the acoustic wave and the dimensions of the confinement structure, there are only two possible effects which an acceleration can have on the crystal resonator:

1. The wave velocity can be perturbed.

2. The confinement dimensions can be changed.

The first effect is primarily a result of the nonlinear elastic behavior of the piezoelectric substrate, while the second effect is primarily a linear mechanical effect.

The portion of the acceleration-induced frequency shift caused by the wave velocity change is typically substantially larger than that caused by the confinement dimension change, and hence the phenomenon is often thought of in the purely nonlinear sense. However, techniques such as aspect-ratio compensation can readily reduce the nonlinear part to levels such that the linear part cannot be ignored.

The linear portion of the problem also causes an asymmetry in the effective material constants such that $\hat{c}_{L\gamma M\alpha} \neq \hat{c}_{\gamma L\alpha M}$ with the important practical implication that both strains and rotations must be considered when determining the acceleration-induced biasing state.

Cause of the Acceleration-Induced Frequency Shift

The driving factor behind an acceleration-induced frequency shift is the deformation of the

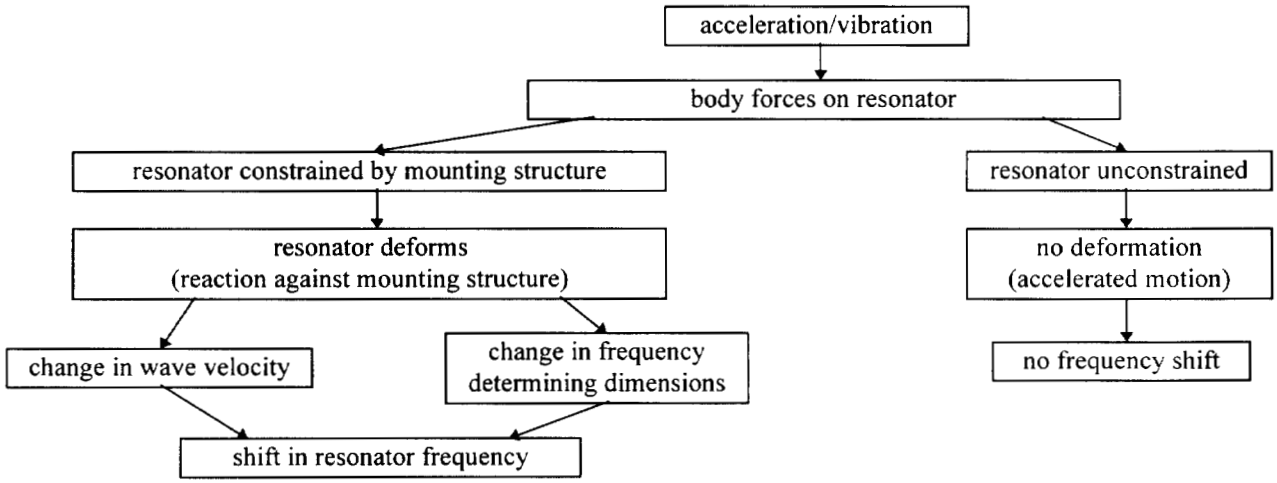

Fig. 3. Flow chart of acceleration effects for constrained and unconstrained resonators.

resonator as it reacts against its mounting structure. This is illustrated in Figure 3, wherein the effects of acceleration on a resonator constrained by a mounting structure are compared to the effects of acceleration on an unconstrained resonator. Acceleration sensitivity is thus a special case of the more fundamental deformation sensitivity of the crystal resonator.

The relationship of acceleration sensitivity to the force-frequency effect, planar stress compensation, etc. is clarified in Table I. All of the listed phenomena are special cases of deformation sensitivity, each distinguished by a particular driving deformation.

Basic Mathematical Approach

How to accurately calculate acceleration sensitivity is now well understood. One can, in theory, directly solve for the frequency under acceleration using a set of differential equations with spatially varying effective elastic constants. It has been shown to be much more efficient to calculate the first perturbation in eigenvalue using the formalism of Tiersten [1]. In this technique, one examines essentially a weighted average of the spatially varying effective elastic constants in that portion of the plate where the mode is driven. It is this effective averaging that is the basis of the various "mode-shaping" proposals recently put forth [2-7].

TABLE I
DEFORMATION SENSITIVITIES

Phenomenon	Deformation Driver
acceleration sensitivity	reaction against mounting structure in response to external acceleration
aging (stress relief)	relaxation of resonator and/or mounting structure
force-frequency effect	diametric compression
planar stress/thermal transient compensation	electrode/substrate interfacial stress

Interpretation of the Perturbation Equations

The basic equations employed in the perturbation approach as developed by Tiersten for the case of purely elastic nonlinearities are

$$\omega = \omega_\mu - \Delta_\mu , \tag{1}$$

$$\Delta_\mu = \frac{H_\mu}{2\omega_\mu} , \tag{2}$$

and

$$H_\mu = -\int_V g^\mu_{\alpha,M} \hat{c}_{L\gamma M\alpha} g^\mu_{\gamma,L} dV , \tag{3}$$

where

$$g^\mu_\gamma = \frac{u^\mu_\gamma}{N_\mu} , \tag{4}$$

and

$$N_\mu^2 = \int_V \rho u_\gamma^\mu u_\gamma^\mu dV . \qquad (5)$$

Equation (1) shows that the frequency under acceleration, ω, is shifted from the unperturbed frequency, ω_μ, by a small amount Δ_μ which can be calculated using equation (2) and "the perturbation integral" of equation (3). The perturbation integral given by equation (3) looks quite complicated but actually has a rather simple interpretation: it is essentially a weighted average of the acceleration induced bias throughout the volume of the quartz plate, where the weighting factor for the averaging is determined by the acoustic mode shape. Equations (4) and (5) provide the necessary normalization of the acoustic mode shape with particle displacements u_γ^μ (Note: the subscript/ superscript μ in (1) through (5) denotes the μ^{th} eigenmode).

The acceleration-induced biasing state is most conveniently written using the material cofactor representation [8]

$$\hat{c}_{L\gamma M\alpha} = k_{L\gamma M\alpha KN}\, w_{N,K} , \qquad (6)$$

where

$$k_{L\gamma M\alpha KN} = c_{L\gamma M\alpha KN} + c_{LMKN}\delta_{\gamma\alpha} + c_{L\gamma KM}\delta_{\alpha N} + c_{LKM\alpha}\delta_{\gamma N} \qquad (7)$$

and $\delta_{\gamma\alpha}$ represents the Kronecker delta. The $w_{N,K}$ factor in equation (6) represents the nine acceleration-induced biasing deformation gradients (N and K take values 1,2,3), and contains all of the required information on how the shape of the crystal plate is deformed by the acceleration. Which $\hat{c}_{L\gamma M\alpha}$ terms are required is determined by the mode of operation, and each $\hat{c}_{L\gamma M\alpha}$ term is the sum of the deformation gradients, each multiplied by the relevant material cofactors $k_{L\gamma M\alpha KN}$ as defined in equation (7). As applied to the calculation of the normal acceleration sensitivity, equations (1) through (3) readily yield

$$\Gamma_i = \frac{1}{8\pi^2 \nu^2 a_i} \int_V g_{\alpha,M}^\mu \hat{c}_{L\gamma M\alpha} g_{\gamma,L}^\mu dV , \qquad (8)$$

where ν denotes the resonant frequency and a_i denotes the external acceleration applied along the x_i direction.

Application of the Perturbation Equations

Equation (8) may be evaluated analytically or numerically. The major advantage of the analytic approach is that it can be used to derive design equations yielding a clear understanding of the functional dependencies of the acceleration sensitivity upon real-world design and fabrication parameters [9, 10]. The numerical approach using finite element techniques to determine the acceleration-induced biasing state has advantages in the analysis of complicated support structures and resonator geometries.

Basic Properties of the Normal Acceleration Sensitivities of Simple Bulk and Surface Modes

It is generally known that the acceleration sensitivity of a given resonator type depends upon the support configuration, choice of substrate material, substrate orientation, substrate dimensions, type of mode, acoustic mode profile, acoustic mode location, etc. In order to obtain a more detailed understanding of the roles these parameters play in determining the acceleration sensitivities of both bulk and surface wave resonators, it is useful to examine the instructive cases of the typically dominant, normal acceleration sensitivities of rotated Y-cut quartz resonators simply supported along rectangular edges.

Cases Considered

The modes considered here are the simple thickness modes described by

$$u_2 = M_a \cdot \sin\left[\beta_p\left(x_2 - \Delta\right)\right] \qquad \text{(AT-cut a-mode)}, \qquad (9a)$$

$$u_3 = M_b \cdot \sin\left[\beta_p\left(x_2 - \Delta\right)\right] \qquad \text{(AT-cut b-mode)}, \qquad (9b)$$

and

$$u_1 = M_c \cdot \sin\left[\beta_p\left(x_2 - \Delta\right)\right] \qquad \text{(AT-cut c-mode)}, \qquad (9c)$$

for

$$\delta - w \le x_1 \le \delta + w , \qquad (9d)$$

$$-h \le x_2 \le +h , \qquad (9e)$$

and

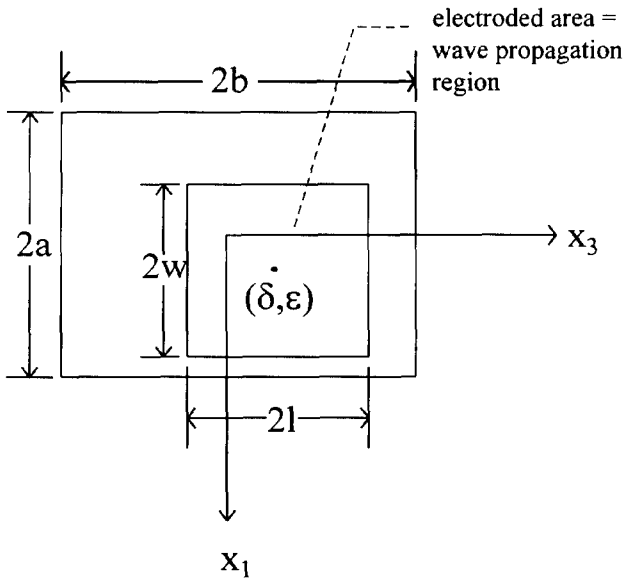

Fig. 4a. BAW device plan view.

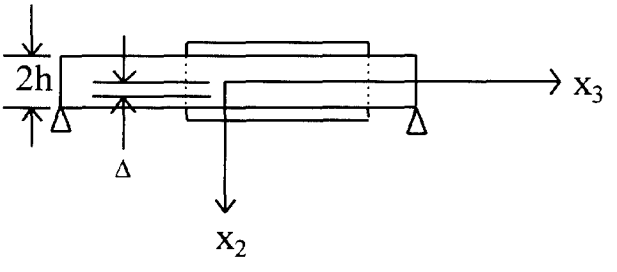

Fig. 4b. BAW device cross-section.

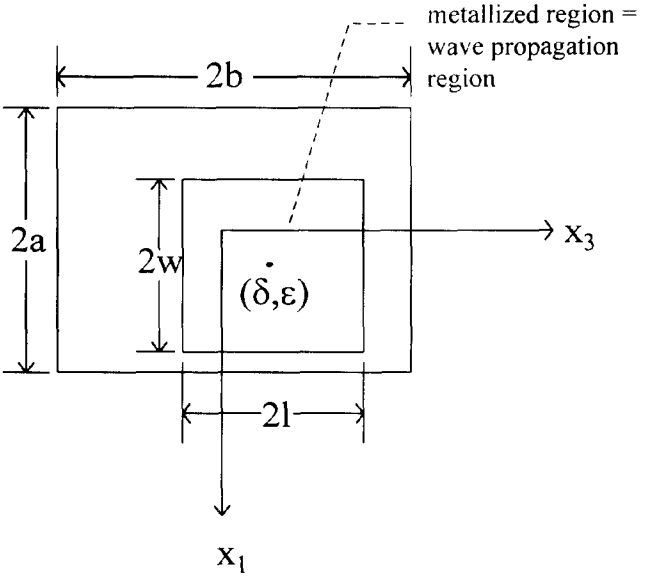

Fig. 5a. STW device plan view.

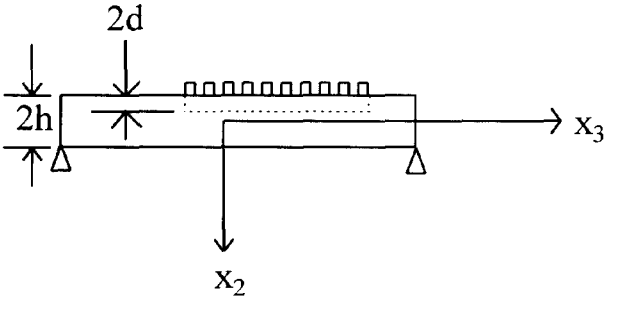

Fig. 5b. STW device cross-section.

$$\varepsilon - l \le x_3 \le \varepsilon + l, \tag{9f}$$

and the simple surface transverse wave (STW) mode described by

$$u_1 = M \cdot \cos\left[\beta(x_3 - \varepsilon)\right], \tag{10a}$$

for

$$\delta - w \le x_1 \le \delta + w, \tag{10b}$$

$$-h \le x_2 \le -h + 2d, \tag{10c}$$

and

$$\varepsilon - l \le x_3 \le \varepsilon + l. \tag{10b}$$

In equations (9) and (10), M represents the modal amplitude, and $\beta \equiv 2\pi/\lambda$ represents the relevant propagation constant. For the BAW modes, we consider $2h = p\lambda/2$ with p=1,3,5,... denoting the harmonic number. For the STW mode, we take the length l of the active area to be a large, integer number of wavelengths and consider $h >> d$.

The modes are considered to be propagating in flat, rotated Y-cut quartz plates simply supported along rectangular edges as illustrated in Figures 4 and 5. For the BAW case, we allow the mode location to be displaced from the central plane of the substrate by a distance Δ along the thickness direction. For both BAW and STW modes, we consider the in-plane mode location to be displaced by (δ,ε) along the rotated X- and Z-axes respectively. The calculated normal acceleration sensitivities are listed in Table II.

TABLE II

NORMAL ACCELERATION SENSITIVITIES OF SIMPLE BULK AND SURFACE MODES FOR ROTATED Y-CUT QUARTZ FLAT PLATE RESONATORS SIMPLY SUPPORTED ALONG RECTANGULAR EDGES

Mode	Normal Acceleration Sensitivity
BAW a-mode	$\sum_{m}^{odd}\sum_{n}^{odd} -\frac{1}{p}\frac{1}{v_a^2}\frac{96}{\pi^5}\frac{a^2b^2\left[\left(m/n\right)E_{2222}b^2+\left(n/m\right)F_{2222}a^2\right]}{\gamma_{11}m^4b^4+\gamma_{33}n^4a^4+(2\gamma_{13}+4\gamma_{55})m^2n^2a^2b^2}\cos(\alpha_m\delta)\sin(2\beta_p\Delta)\cos(\kappa_n\varepsilon)\frac{\sin(\alpha_m w)}{\alpha_m w}\frac{1}{h}\frac{\sin(\kappa_n l)}{\kappa_n l}$
BAW b-mode	$\sum_{m}^{odd}\sum_{n}^{odd} -\frac{1}{p}\frac{1}{v_b^2}\frac{96}{\pi^5}\frac{a^2b^2\left[\left(m/n\right)E_{2323}b^2+\left(n/m\right)F_{2323}a^2\right]}{\gamma_{11}m^4b^4+\gamma_{33}n^4a^4+(2\gamma_{13}+4\gamma_{55})m^2n^2a^2b^2}\cos(\alpha_m\delta)\sin(2\beta_p\Delta)\cos(\kappa_n\varepsilon)\frac{\sin(\alpha_m w)}{\alpha_m w}\frac{1}{h}\frac{\sin(\kappa_n l)}{\kappa_n l}$
BAW c-mode	$\sum_{m}^{odd}\sum_{n}^{odd} -\frac{1}{p}\frac{1}{v_c^2}\frac{96}{\pi^5}\frac{a^2b^2\left[\left(m/n\right)E_{2121}b^2+\left(n/m\right)F_{2121}a^2\right]}{\gamma_{11}m^4b^4+\gamma_{33}n^4a^4+(2\gamma_{13}+4\gamma_{55})m^2n^2a^2b^2}\cos(\alpha_m\delta)\sin(2\beta_p\Delta)\cos(\kappa_n\varepsilon)\frac{\sin(\alpha_m w)}{\alpha_m w}\frac{1}{h}\frac{\sin(\kappa_n l)}{\kappa_n l}$
STW	$\sum_{m}^{odd}\sum_{n}^{odd} \frac{1}{v_{STW}^2}\frac{96}{\pi^4}\frac{a^2b^2\left[\left(m/n\right)E_{3131}b^2+\left(n/m\right)F_{3131}a^2\right]}{\gamma_{11}m^4b^4+\gamma_{33}n^4a^4+(2\gamma_{13}+4\gamma_{55})m^2n^2a^2b^2}\cos(\alpha_m\delta)\cos(\kappa_n\varepsilon)\frac{\sin(\alpha_m w)}{\alpha_m w}\frac{1}{h}\frac{\sin(\kappa_n l)}{\kappa_n l}$

NOTE: $\alpha_m \equiv \frac{m\pi}{2a}$; $\kappa_n \equiv \frac{n\pi}{2b}$; $E_{L\gamma M\alpha}$ and $F_{L\gamma M\alpha}$ as defined in [9,10]; $\beta_p \equiv \frac{2\pi}{\lambda} = \frac{p\pi}{2h}$

Interpretation of the Solutions

The various terms in the simplified solutions presented in Table II clarify the basic properties of the normal acceleration sensitivities as follows:

$\sum_{m}^{odd}\sum_{n}^{odd}$ - the summations reflect the fact that the flexural deformation is described by a Fourier series expansion

+/− - reflects that the sign of the frequency shift can be correctly determined

$\frac{1}{p}$ - proportional to inverse of the harmonic number for BAW modes

$\frac{1}{v_{mode}^2}$ - proportional to inverse square of the modal velocity

$\frac{96}{\pi^4}$ or $\frac{96}{\pi^5}$ - proportionality constant depends on whether the device is a bulk or surface wave resonator

quotient - directly proportional to complicated sum of linear and nonlinear stiffnesses via $E_{L\gamma M\alpha}$ and $F_{L\gamma M\alpha}$

- inversely proportional to linear stiffnesses controlling flexural rigidity via Voigt's anisotropic plate stiffnesses γ_{11}, γ_{33}, γ_{13}, and γ_{55}

- net proportionality to the square of the lateral dimensions, i.e., proportional to area of the major surface

- $\left[\left(m/n\right)E_{L\gamma M\alpha}b^2+\left(n/m\right)F_{L\gamma M\alpha}a^2\right]$ enables aspect-ratio compensation when $E_{L\gamma M\alpha}$ and $F_{L\gamma M\alpha}$ are of opposite sign

$\cos(\alpha_m\delta)$ - proportionality to an x_1-direction mode center offset

$\sin(2\beta_p\Delta)$ - proportionality to an x_2-direction mode center offset for BAW modes

$\cos(\kappa_n\varepsilon)$ - proportionality to an x_3-direction mode center offset

$\frac{\sin(\alpha_m w)}{\alpha_m w}$ - proportionality to the x_1-direction mode profile

$\frac{1}{h}$ - inversely proportional to plate thickness, with no proportionality to the x_2-direction mode profile

$\frac{\sin(\kappa_n\varepsilon)}{\kappa_n\varepsilon}$ - proportionality to the x_3-direction mode profile

Similarities and Differences between the Bulk and Surface Wave Solutions

The properties of the BAW and STW solutions are essentially identical with regard to most design parameters, particularly with respect to in-plane variations such as mode center offset. The differences in sign and the additional $1/\pi$ factor in the BAW case are not significant with regard to the nature and properties of the solutions.

There are two factors which appear only in the BAW solution. First, the consideration of harmonic operation in the BAW case leads to a factor of 1/p not found in the STW case, where only fundamental mode operation is considered. Second, the BAW case includes a term $\sin(2\beta\Delta)$ causing the BAW acceleration sensitivity to be proportional to the thickness direction mode center offset, whereas the STW acceleration sensitivity has no dependence upon the thickness direction properties of the acoustic mode shape.

The BAW and STW acceleration sensitivities both depend upon the plate thickness. In the BAW case, the thickness is also the frequency determining dimension. As a result, there is a net frequency dependence of the BAW acceleration sensitivity for scaled designs such a microresonators.

Additional Discussion of the BAW Solutions

The BAW acceleration sensitivity depends upon the harmonic number in two ways. First, there is a direct 1/p dependence upon harmonic number p. Second, the propagation constant $\beta_p = 2\pi/\lambda = p\pi/2h$ appears in the $\sin(2\beta_p\Delta)$ term, which may be rewritten as $\sin(p\times 2\beta_1\Delta)$. The direct 1/p dependence tends to decrease the acceleration sensitivity with increasing harmonic. If the thickness direction mode center offset Δ is taken to be the same for the various harmonics, then the $\sin(2\beta_p\Delta)$ term increases with increasing harmonic, tending to increase the acceleration sensitivity with increasing harmonic. Published experimental results on the harmonic dependence of acceleration sensitivity indicate an initial decrease in acceleration sensitivity with increasing harmonic number, after which the acceleration sensitivity is essentially constant or slightly increased [11].

The qualitative effects of energy trapping on the acceleration sensitivity can be understood readily from the solutions presented here by taking the case of a more tightly trapped mode to correspond to an increased modal amplitude M_a, M_b, or M_c in conjunction with a decrease in the active area given by $2l\times 2w$.

Extension to In-Plane Acceleration Sensitivities

The various terms in the solutions listed in Table II arise from specific aspects of the phenomenon. For example, the Fourier series expansion, direct proportionality to substrate area, inverse proportionality to substrate thickness, and inverse proportionality to the stiffnesses governing flexure are all reflections of the flexural biasing deformation. By considering the similarities and differences between the cases of normal and in-plane accelerations, the results given for the normal acceleration sensitivities readily can be extended to the understanding of the in-plane acceleration sensitivities.

Advanced Properties of More Complicated Modes

Additional insights into the fundamental nature of acceleration sensitivity are obtained from the analysis of more complicated modes such as trapped energy modes.

Limitations of the Simple Mode Analyses

The simple mode solutions as listed in Table II, while instructive, are exact only for the considered cases of uniform amplitude, pure-mode propagation (only u_1 or u_2 or u_3 present). In reality, the modes driven in practical resonators have spatially varying amplitudes and components of the particle displacement along all three axes (u_1, u_2, and u_3 all present). Such modes lead to solutions with slightly more complicated functional behaviors, and to solutions that are the sum of multiple terms. This is illustrated in Table III wherein the simple mode STW solution is compared to the trapped energy STW solution from [9]. Additional complications are introduced in the Rayleigh wave case where the surface acoustic wave (SAW) mode is composed of the sum of four partial waves.

It is important to note that the simple mode solutions correspond to the dominant terms in the trapped energy solutions. Hence, where aspect-ratio compensation is not used (as, for example, in 4-point mounted BAW resonators), the simple mode solutions provide useful guidance for the design of 10^{-10}/g performance devices.

TABLE III

COMPARISON OF SIMPLE AND TRAPPED ENERGY STW MODE NORMAL ACCELERATION SENSITIVITIES

Mode Type	Normal Acceleration Sensitivity
Simple	$\sum_{m}^{odd}\sum_{n}^{odd}\frac{1}{v_{STW}^2}\frac{96}{\pi^4}\frac{a^2b^2\left[\left(m/n\right)E_{3131}b^2+\left(n/m\right)F_{3131}a^2\right]}{\gamma_{11}m^4b^4+\gamma_{33}n^4a^4+\left(2\gamma_{13}+4\gamma_{55}\right)m^2n^2a^2b^2}\cos\left(\alpha_m\delta\right)\cos\left(\kappa_n\varepsilon\right)\frac{\sin\left(\alpha_m w\right)}{\alpha_m w}\frac{1}{h}\frac{\sin\left(\kappa_n l\right)}{\kappa_n l}$
Trapped Energy	$\sum_{m}^{odd}\sum_{n}^{odd}-\frac{1}{v^2}\frac{24}{\pi^2}\left[\frac{a^2b^2\left[\left(m/n\right)E_{3131}b^2+\left(n/m\right)F_{3131}a^2\right]}{\gamma_{11}m^4b^4+\gamma_{33}n^4a^4+\left(2\gamma_{13}+4\gamma_{55}\right)m^2n^2a^2b^2}\right]\cos\left(\alpha_m\delta\right)\cos\left(\kappa_n\varepsilon\right)$ $*\left[\frac{2\sin\left(\alpha_m w\right)}{\alpha_m w}+\frac{\sin\left(\left\{2\chi+\alpha_m\right\}w\right)}{\left(2\chi+\alpha_m\right)w}+\frac{\sin\left(\left\{2\chi-\alpha_m\right\}w\right)}{\left(2\chi-\alpha_m\right)w}\right]\left[\left(\frac{1}{h}\right)\cdot\left(\frac{1-2\xi h\cdot\coth\left(2\xi h\right)}{2\xi h}\right)\right]$ $*\left\{\left[\frac{2\sin\left(\kappa_n s\right)}{\kappa_n s}+\frac{\sin\left(\left\{2\beta+\kappa_n\right\}s\right)}{\left(2\beta+\kappa_n\right)s}+\frac{\sin\left(\left\{2\beta-\kappa_n\right\}s\right)}{\left(2\beta-\kappa_n\right)s}\right]+\left[\frac{2\left\{2\zeta\cos\left(\kappa_n s\right)-\kappa_n\sin\left(\kappa_n s\right)\right\}}{\left[4\zeta^2+\kappa_n^2\right]s}\right.\right.$ $\left.\left.-\frac{2\zeta\cos\left[\left(2\beta+\kappa_n\right)s\right]-\left(2\beta+\kappa_n\right)\sin\left[\left(2\beta+\kappa_n\right)s\right]}{\left[4\zeta^2+\left(2\beta+\kappa_n\right)^2\right]s}-\frac{2\zeta\cos\left[\left(2\beta-\kappa_n\right)s\right]-\left(2\beta-\kappa_n\right)\sin\left[\left(2\beta-\kappa_n\right)s\right]}{\left[4\zeta^2+\left(2\beta-\kappa_n\right)^2\right]s}\right]\right\}$ $*\left[1+\frac{1}{2\zeta s}+\left(\frac{\beta\zeta}{\beta^2+\zeta^2}\right)\frac{\cos\left(2\beta s\right)}{2\beta s}+\left(\frac{\zeta^2}{\beta^2+\zeta^2}\right)\frac{\sin\left(2\beta s\right)}{2\beta s}\right]^{-1}$ + 12 other smaller terms

Important Properties of the Smaller Terms

The dominant term in the trapped energy solutions can be minimized readily through the use of aspect-ratio compensation, in which case the properties of the smaller terms must be considered. The most significant difference in the properties of the smaller terms as compared to the dominant term is in their proportionalities to in-plane mode center offsets. Whereas the dominant term is proportional to the cosines of the mode center offsets, the various smaller terms have combinations and permutations of sine and cosine proportionalities.

"Mode Shaping"

Techniques for minimizing the acceleration sensitivity through control of the acoustic mode shape have been proposed by Ballato [2], EerNisse, et al. [3-6], and Smythe and Horton [7]. The solutions presented in Table II clarify the distinctly different roles of mode shape, i.e. "profile", and mode location. Note that the theoretical zero acceleration sensitivity of the ideal (symmetric), rotated Y-cut simple BAW resonator considered here arises solely from the thickness direction symmetry. While the trapped energy resonator will, in fact, require a full three-dimensional symmetry to obtain zero acceleration sensitivity, the dominant and hence most important symmetry in practice in the AT-cut is not the in-plane symmetry but rather the thickness-direction symmetry (see, for example, [12]).

Other Types of Resonators

The discussions of the fundamental nature of acceleration sensitivity and simple mode results also

clarify important aspects of the phenomenon in other types of resonators.

BAW Microresonators

The simple mode solutions for BAW resonators indicate potentially superior acceleration sensitivities for BAW microresonators, provided that fabrication tolerances are properly controlled. For scaled designs (i.e., similar diameter- and electrode-to-thickness ratios, relative dimensional tolerances, etc.) there is a net 1/f dependence of the acceleration sensitivity. Hence a 10^{-10}/g design at 10 MHz could yield 10^{-12}/g when implemented as a 1 GHz microresonator.

Dielectric Resonators

The basic principle of operation of a generic resonator as illustrated in Figure 2 also applies to the dielectric resonator. Consequently, the fundamental nature of acceleration sensitivity in the dielectric resonator is essentially the same as that for the crystal resonator, i.e., there are only two possible effects which an acceleration can have on the dielectric resonator:

1. The wave velocity can be perturbed.

2. The confinement dimensions can be changed.

For the dielectric resonator, the wave velocity change is a result of the nonlinear piezooptic effect, while the confinement dimension change is primarily a linear mechanical effect. As for the crystal resonator, the driving factor behind the acceleration-induced frequency shift is the deformation of the dielectric resonator as it reacts against its mounting structure [13].

Measurement and Specification

Understanding that the deformation of the resonator is the driving factor behind acceleration sensitivity highlights a critical but as yet unaddressed issue in measurement and specification: *the measurement and specification of acceleration sensitivity are only meaningful with respect to a well defined mechanical interface.*

To illustrate this point, consider the simple mode solutions presented in Table II. These solutions assume that the resonator supports remain perfectly planar under acceleration, as might be the case in practice for a resonator attached to a sufficiently thick ceramic substrate. However, in the vast majority of practical applications, the mounting "plane" of the resonator and/or oscillator is substantially distorted under acceleration. A common example would be a resonator or oscillator attached to a much larger printed circuit board. In this case, the resonator deformation is the sum of the "free" deformation of the ideal resonator plus the defined strain imposed by the deformation of the circuit board. Hence the specification, design, and measurement of resonators for such an application must account for the defined strain imposed by the circuit board.

Conclusions

The fundamental nature of acceleration sensitivity is now well understood. The driving factor behind the acceleration-induced frequency shift is the deformation of the resonator. The acceleration sensitivities of practical resonators can be accurately calculated using the perturbation theory of Tiersten.

The perturbation equations have been solved analytically to obtain reliable design equations for BAW, SAW, and STW resonators. The design equations clarify the functional dependencies of the acceleration sensitivities on the full range of crystal resonator design and fabrication parameters.

References

[1] H. F. Tiersten, "Perturbation Theory for Linear Electroelastic Equations for Small Fields Superposed on a Bias," Journal of the Acoustical Society of America, vol. 64, no. 3, pp. 832-837, September 1978.

[2] A. Ballato, "Method of Making an Acceleration Hardened Resonator," U.S. Patent 4,836,882, June 6, 1989, 5 pp.

[3] E. P. EerNisse and R. W. Ward, "Crystal Resonator With Low Acceleration Sensitivity and Method of Manufacture Thereof," U.S. Patent 4,837,475, June 6, 1989, 9 pp.

[4] E. P. EerNisse, R. W. Ward, and O. L. Wood, "Crystal Resonator With Low Acceleration Sensitivity and Method of Manufacture Thereof," U. S. Patent 4,935,658, June 19, 1990, 8 pp.

[5] E. P. EerNisse, R. W. Ward, and O. L. Wood, "Method of Manufacturing Crystal Resonators

Having Low Acceleration Sensitivity," U.S. Patent 5,022,130, June 11, 1991, 9 pp.

[6] E. P. EerNisse, R. W. Ward, and O. L. Wood, "Crystal Resonator with Low Acceleration Sensitivity and Method of Manufacture Thereof," U.S. Patent 5,168,191, December 1, 1992, 8 pp.

[7] R. C. Smythe and W. H. Horton, "Adjustment of Resonator G-Sensitivity by Circuit Means," in Proceedings of the 44th Annual Frequency Control Symposium, May 1990, pp. 437-443.

[8] J. A. Kosinski and A. Ballato, "Designing for Low Acceleration Sensitivity," IEEE Transactions on Ultrasonics, Ferroelectrics, and Frequency Control, Special Issue on Applications, vol. 40, no. 5, pp. 532-537, September 1993.

[9] J. A. Kosinski, J. T. Stewart, A. Ballato, and R. Almar, "An Analysis of the Normal Acceleration Sensitivity of Rotated Y-cut Quartz Surface Transverse Wave Resonators Simply Supported Along Rectangular Edges," in Proceedings of the 1995 IEEE International Frequency Control Symposium, June 1995, pp. 486-493.

[10] J. A. Kosinski, "Acceleration Sensitivity of SAW and STW Devices," in 1995 IEEE International Ultrasonics Symposium Proceedings, November 1995, pp. 187-196.

[11] R. L. Filler, J. A. Kosinski, and J. R. Vig, "Further Studies on the Acceleration Sensitivity of Quartz Resonators," in Proceedings of the 37th Annual Frequency Control Symposium, June 1983, pp. 265-271.

[12] R. L. Filler, J. A. Kosinski, and J. R. Vig, "The Effect of Blank Geometry on the Acceleration Sensitivity of AT- and SC-cut Quartz Resonators," in Proceedings of the 36th Annual Frequency Control Symposium, June 1982, pp. 215-219.

[13] P. C. Y. Lee, J. D. Yu, and A. Ballato, "Effect of Stress on Guided EM Waves in Anisotropic Dielectric Plates," in Proceedings of the 1993 IEEE International Frequency Control Symposium, June 1993, pp. 461-471.